Spontaneous Helicity of a Polymer with Side Loops Confined to a Cylinder

Debasish Chaudhuri*
FOM Institute AMOLF, Science Park 104, 1098XG Amsterdam, Netherlands
Indian Institute of Technology Hyderabad, Yeddumailaram 502205, Andhra Pradesh, India

Bela M. Mulder†
FOM Institute AMOLF, Science Park 104, 1098XG Amsterdam, Netherlands
(Received 30 November 2011; revised manuscript received 3 May 2012; published 27 June 2012)

Inspired by recent experiments on the spatial organization of bacterial chromosomes, we consider a type of ''bottle-brush'' polymer consisting of a flexible backbone chain, to which flexible side loops are connected. We show that such a model with an open linear backbone spontaneously adopts a helical structure with a well-defined pitch when confined to small cylindrical volume. This helicity persists over a range of sizes and aspect ratios of the cylinder, provided the packing fraction of the chain is suitably large. We analyze these results in terms of the interplay between the effective stiffness and actual intrachain packing effects caused by the side loops in response to the confinement.

DOI: 10.1103/PhysRevLett.108.268305 PACS numbers: 82.35.Pq, 87.15.ap, 87.16.Sr, 89.75.Fb

That confinement can dramatically influence the properties of nonideal polymers has already been appreciated theoretically for a long time. Scaling arguments suggest that when a confining dimension D becomes smaller than the natural size of a linear polymer, typically given by its radius of gyration R, the polymer, rather than behaving like a single coherent ''blob'' of size R, effectively becomes a string of blobs of size D [1], signaling a crossover to lower-dimensional behavior. The experimental exploration of this regime, however, is difficult using synthetic polymers, whose typical radii of gyration are in the nm regime and, moreover, tend to be highly polydisperse in length [2]. Fortunately, nature provides us with an important class of model polymers in the form of DNA. To start with, DNA is produced with almost perfect length control. A well-studied example *in vitro* is purified λ-phage DNA, which contains exactly 48502 base pairs and has a length of 16.5 μm and a radius of gyration of 2.1 μm. Using biochemical tools, this length can be scaled to multiples of this unit. Moreover, DNA can readily be fluorescently labeled. These two properties of DNA were exploited in a number of recent experiments aimed at studying the behavior of polymers confined to nanofluidic channels [3–5].

More importantly, *in vivo* DNA in the form of chromosomes is almost invariably strongly confined. The paradigmatic case is the 1.5-mm long circular chromosome of the bacterium *E. coli*, which is confined to a cylindrical volume of diameter $\sim$0.8 μm and length varying between 2–4 μm. Over the past few years, there has been increasing interest in understanding the details of the chromosomal configuration in *E. coli* and its implications for the, as yet far from fully understood, mechanism of sister-chromosome segregation prior to division [6–8]. Strikingly, recent microscopic observations have shown that bacterial chromosomes can exhibit a helical spatial density distribution within the cellular confinement, with a pitch-length in the order of a fraction of the cell length [9,10].

The idea that a helical arrangement of a linear filament under certain conditions provides the highest density packing was already proposed by Maritan *et al.* [11] over a decade ago. The latter work, however, was purely based on geometrical considerations and did not address whether such configurations are stable for microscopic filaments under thermodynamic conditions. Here, we ask to what extent such configurations can indeed arise as finite-temperature equilibrium configurations of real polymers with short range interactions and, hence, provide clues to potential purely physical mechanisms contributing to the novel global configurations of bacterial chromosomes. To that end, we take a cue from the fact that the structure of a typical bacterial chromosome is not simply that of a closed linear polymer chain. The combined effects of supercoiling, due to a globally maintained undertwist of the DNA, the action of a number of chromosome remodeling proteins, or even electrostatic ''zippering'' can cause loops in the DNA [12], indicating that a more complex structural picture is needed. Although in reality the dynamics of the formation and the statistics of such loops are likely to be highly complex, almost certainly involving polydispersity in loop sizes and topological entanglements, we chose to focus on arguably the simplest model of a polymer ''dressed'' by a cloud of loops, i.e., a backbone chain to which side loops of equal size are attached at regular spacing. The same model has recently also been discussed by Reiss, Fritsche, and Heermann [13], who have studied its behavior in the absence of confinement effects. This type of polymer model is similar to the so-called ''bottle-brush'' polymers, extensively studied by Binder and co-workers [14–16]. The latter work has shown that such polymers develop a local resistance to bending due to the entropic

repulsion between the side chains [17]. This effective stiffening, combined with intrachain packing effects within the cylindrical confinement, leads, as we will show in the following, to the spontaneous formation of helical configurations, which, however, do not appear to be optimal in the sense of Ref. [11].

Our model polymers are of the bead-spring type, with consecutive beads attached to each other by a harmonic spring $V_b = (A/2)(\mathbf{d_i} - \sigma\mathbf{u_i})^2$, where $\mathbf{d_i} = \mathbf{r}_{i+1} - \mathbf{r}_i$, $\mathbf{r_i}$ is the position of ith bead, σ the equilibrium bond length, and $\mathbf{u}_i = \mathbf{d_i}/|\mathbf{d_i}|$ is the local tangent vector to the chain. Nonbonded beads repel each other through the Weeks-Chandler-Andersen (WCA) potential [18] $V_{\mathrm{WCA}} = 4\epsilon[(\sigma/r_{ij})^{12} - (\sigma/r_{ij})^6 + 1/4]$ if the intermonomer separation $r_{ij} < 2^{1/6}\sigma$ else $V_{\mathrm{WCA}} = 0$, where ϵ and σ set the energy and length scale of the system, respectively. We use $A = 100\epsilon$. The interaction of all beads, irrespective of whether they belong to the main chain or side loops, with the confining walls (the top and bottom surfaces, as well as the cylindrical side surface) are modeled through $V_{\mathrm{wall}} = 2\pi\epsilon[(2/5)(\sigma/r_{iw})^{10} - (\sigma/r_{iw})^4 + 3/5]$ if the distance of the ith monomer from a wall $r_{iw} < \sigma$ and $V_{\mathrm{wall}} = 0$ otherwise. We simulate this system employing a velocity-Verlet molecular dynamics scheme in the presence of a Langevin thermostat fixing the temperature at $k_BT = 1$ as implemented by the ESPResSo package [19].

We first consider a polymer composed of a linear backbone chain of length $l_b = 200\sigma$ to which side loops of length $l_s = 40\sigma$ are attached at every backbone monomer of the main chain. This polymer is confined to a cylinder of length $L = 50.75\sigma$ and diameter $D = 29.5\sigma$, yielding a monomer packing fraction of $\eta = 23.8\%$. In Fig. 1, we show a typical equilibrium configuration of this polymer, which evidently displays a marked helical ordering of the backbone chain. The degree of helical ordering can be quantified by considering the tangent-tangent correlation function $\langle \mathbf{u}(s) \cdot \mathbf{u}(0) \rangle$, between two arbitrary tangent vectors separated by a distance $s = i\sigma$ with $i = 0, 1, \ldots, 200$. The Fourier transform of this quantity yields a structure function $S(q)$ with a peak at a dimensionless wave number $q_{\mathrm{max}} = l_b/\lambda_{\mathrm{max}}$, where λ_{max} is the pitch of the helix measured along the backbone chain. The height of the structure function at its maximum is a relative measure of the degree of helicity, while the width of the peak is indicative of the statistical dispersion of the structure.

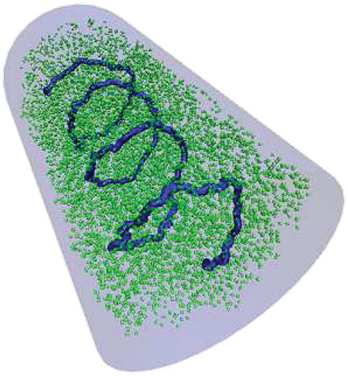

FIG. 1 (color). Helical equilibrium structure for a backbone chain of length $l_b = 200\sigma$ [blue thick line] to which side-loops of length $l_s = 40\sigma$ are attached at each backbone monomer. The polymer is confined within a cylinder of length $L = 50.75\sigma$ and diameter $D = 29.5\sigma$. The side-loop monomers are shown as transparent green beads.

Figure 2 shows the correlation function and the corresponding structure function for this polymer, as we vary the diameter of the confining cylinder. This shows that the helical pitch is relatively robust against changes in the diameter, although a slight decrease in the amplitude is apparent as we increase the diameter. Only for the largest diameter, when both the degree of confinement as well as the overall packing fraction are significantly decreased, do we see a preference for a more longitudinal packing of the main chain. The helical pitch is equally robust against reduction of the cylinder length, keeping the diameter constant. However, at very high compression the structural relaxation becomes extremely slow, and the polymer configuration gets kinematically trapped into random close packed structures (data not shown).

Maritan *et al.* [11] have suggested that the optimally packed helical string is uniquely characterized by the critical pitch-to-radius ratio of $c \equiv p/r = 2.512$. Calculating the mean radius r_m of the helices corresponding to Fig. 2 yields values of this ratio of $c = \lambda_{\mathrm{max}}/r_m = 3.27, 2.5, 1.8$ for $D/\sigma = 14.68, 19.85, 29.5$, respectively. This shows that, while the pitch-to-radius ratio of these equilibrium polymers is of the same order as the ideal geometrical ones, in this case both the details of the polymer structure

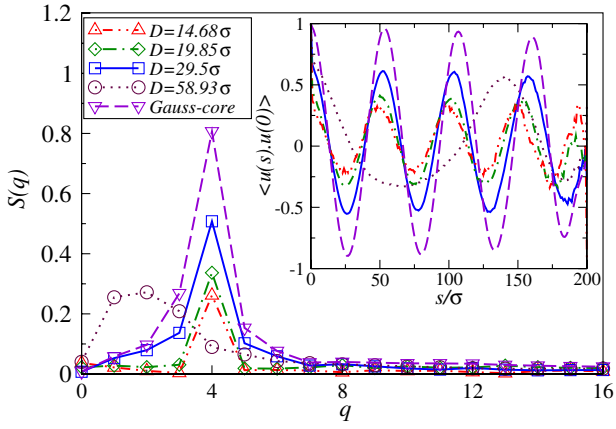

FIG. 2 (color online). The tangent-tangent correlation (inset) and its Fourier transform for the polymer shown in Fig. 1. The correlation function is oscillatory, with the periodicity captured by the peak in the structure factor at $q_p = 4$ for $D/\sigma = 14.68$, 19.85, 29.5, and $q_p = 2$ for $D/\sigma = 58.93$. Also shown are the corresponding results for a main-chain polymer with an effective Gaussian-core mimicking the effect of inter-side-chain repulsion [cf. Fig. 4(b)].

and the nature of the confinement are expected to play a role.

We now argue that the helical arrangement is stabilized by two effects. The first is the effective stiffness induced in the backbone by the presence of side loops. To quantify this intrinsic effect in the absence of confinement, we study a *free* polymer of length $l_b = 500$, with side loops of the same length as before, $l_s = 40\sigma$, grafted at each backbone monomer. Although for a very long backbone ($l_b \gg l_s$) one expects the exponent b, which governs the mean-square separation between monomers at a distance s along the backbone through the scaling $\langle r(s)^2 \rangle \sim s^{2b}$, to reproduce the value $b = 3/5$ of a simple self-avoiding polymer, we find at the shorter length scales relevant to our confined polymer, a much higher value of $b = 0.97$ (Fig. 3, inset). At the same time, the tangent-tangent correlation $\langle \mathbf{u}(s).\mathbf{u}(0) \rangle$ (Fig. 3) shows an extremely weak power-law decay $s^{-\alpha}$ with $\alpha = 0.06$, which satisfies the generic scaling rule $\alpha = 2 - 2b$. The small value of the exponent $\alpha \ll 1$ suggests that at these relatively short length scales the backbone is characterized by a significant effective stiffness, even close to that of a of a rigid rod for which $b = 1$. The algebraic nature of the correlation decay, however, precludes a simple interpretation in terms of an intrinsic length, in contrast to the persistence length of a chain with intrinsic resistance to bending. Nevertheless, it is intuitively clear that there is a free-energy cost associated with local deformations of the backbone caused by the changes induced in the side-loop packing. For comparison, we note that the end-to-end distance measured for our backbone with $l_b = 500$, which we determined to be $R \approx 413\sigma$, would be reproduced by a wormlike chain with persistence length $P \approx 391\sigma$ [20] comparable to the contour length.

However, backbone stiffness alone is not sufficient to explain the emergent helicity. Although earlier work has shown that a persistent chain confined to the surface of a cylinder can adopt helical conformation [21], a persistent chain confined to the volume of a cylinder does not. We confirm this by simulating a wormlike chain (WLC) of length $l_b = 200\sigma$ with a persistence length of $P = 2l_b$, close to the effective value determined above for the free polymer. A typical equilibrium structure of the confined WLC is shown in Fig. 4, which clearly displays the tendency of such a chain to align itself with the long axis of the cylinder, without much internal structure developing, also supported by an analysis of the tangent-tangent correlations (see Supplemental Material [22]).

This negative result for the persistent chain points to the importance of the packing of the side loops in stabilizing the helical structure. One could naively expect that the interactions between the side loops cause an additional effective soft repulsion between the backbone monomers with a range determined by the radius of gyration of the side loops. This repulsion has a dual role; as we have shown above, it stiffens the backbone at short length scales, but at long length scales it acts to keep distant parts of the backbone apart, effectively thickening the backbone to a soft tube. To assess the validity of this latter idea, we consider a chain whose monomers, apart from interacting through the short range WCA potential, also interact with an effective Gaussian-core interaction

$$\beta V_{\mathrm{gc}}(r) = a \exp[-(r/w)^2] \tag{1}$$

intended to mimic, as simply as possible, the soft repulsion between the side loops. Bolhuis *et al.* showed that, in free space, the effective interaction between two linear polymers of the same length can be approximated by the above expression with $a \sim 2$ and $w = R_g$, the radius of gyration of the individual polymers [23]. While it is well known that the free-energy cost of overlap between two polymers in free space is independent of polymer size [24–26], the blob picture of polymers suggests that their overlap free energy will become a linear function of polymer length [7] when the chains are strongly confined. We, therefore, take the interaction strength $a = 40$ to mimic the densely-packed side loops of size $l_s = 40\sigma$. From our simulations of side-loop coupled backbone, we found the mean radius of

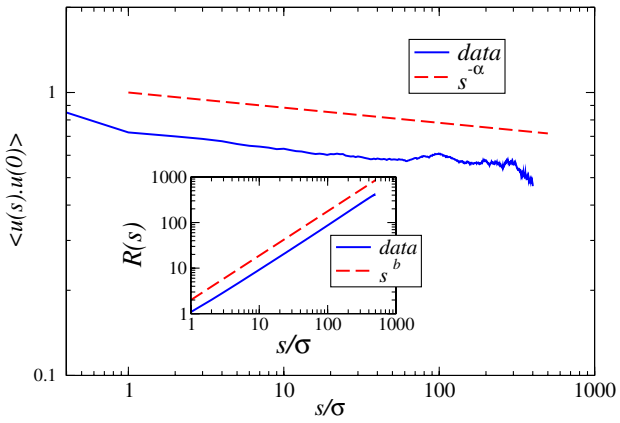

FIG. 3 (color online). The tangent-tangent correlation shows a weak power-law decay $s^{-\alpha}$ with $\alpha = 0.06$. Inset: power-law growth of distance between two segments $R(s) = \sqrt{\langle r(s)^2 \rangle} \sim s^b$ with $b = 0.97$.

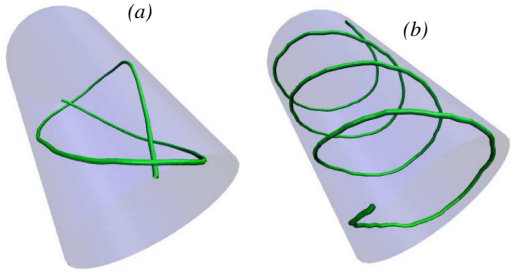

FIG. 4 (color online). (a) Self-avoiding WLC and (b) self-avoiding Gaussian-core polymer within a cylinder. The chain has contour length $l_b = 200\sigma$, and for the WLC polymer the persistence length $P = 2l_b$. The confining cylinder is of length $L = 50.75\sigma$ and diameter $D = 29.5\sigma$ for both (a) and (b).

gyration $R_g = 2.95\sigma$ of the side loops of length $l_s = 40\sigma$. However, due to the repulsive interactions with the backbone monomers, the center of mass of the loops is offset from the backbone. We, therefore, extracted the distribution of the center of mass of the side loops with respect to their attachment point on the backbone in the plane perpendicular to the local tangent direction along the chain (see Fig. S1 in the Supplemental Material [22]). This distribution has a sharp maximum at a distance of approximately 4σ from the backbone chain. This result also shows that indeed the density distribution of the side-loop monomers is structured in a manner consistent with the thickened tube picture alluded to above. We, therefore, took the size parameter characterizing the range of the interaction between the side loops in the effective potential centered on the backbone monomers V_{gc} to be $w \simeq R_g + 4\sigma = 6.95\sigma$. This effective interaction between the monomers was then added to the WCA potential, governing the nonbonded repulsive interactions, for a linear chain of length $l_b = 200\sigma$ confined within a cylinder of diameter $D = 29.5\sigma$ and length $L = 50.75\sigma$. As Fig. 4(b) shows, this effective potential reproduces the helical equilibrium structures of the polymer remarkably well. The structure factor displays a maximum at the same helical pitch value $l_b/4 = 50\sigma$ as the original simulations and reproduces the oscillations of the tangent-tangent correlation function (Fig. 2) with only a slight global phase shift. The amplitude of the oscillations (and, hence, that of the structure factor) is somewhat larger for the effective potential, but this is probably due to an overestimate of the interaction strength a.

Finally, we enquire into what happens if the backbone is a ringlike polymer, inspired by the fact that the chromosome of *E. coli* is circular. To that end, we simulated a polymer with a circular backbone with $l_b = 400\sigma$ and side loops of length $l_s = 20\sigma$, trapped within a cylinder of length $L = 50.4\sigma$ and diameter $D = 33.5\sigma$. The packing fraction of the monomers is $\eta = 18.9\%$, comparable to the one in the simulation of the linear backbone polymer. Figure 5 shows that in this case the backbone loop is now organized into two parallel helices running along the long axis of the cylinder. As is evident from the snapshot, and corroborated by the analysis of the tangent-tangent correlations (Fig. S3 in Supplemental Material [22]), the degree of helicity is reduced as compared to the linear backbone case, due to the smaller side-loop length, but nevertheless remains significant.

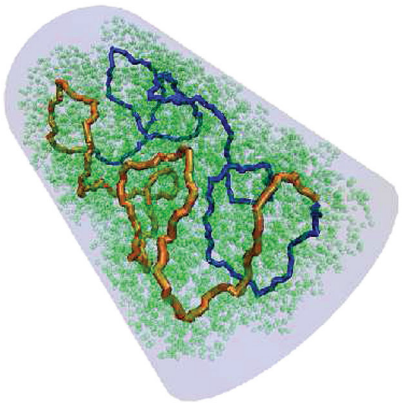

FIG. 5 (color). Equilibrium structure for a circular backbone chain of length $l_b = 400\sigma$, with side loops of length $l_s = 20\sigma$ attached to each backbone monomer. The polymer is confined within a cylinder of length $L = 50.4\sigma$ and diameter $D = 33.5\sigma$. The splitting of the backbone into two parallel linearized branches is highlighted by using two color codes, orange and blue, for the branches. The side-loop monomers are shown as transparent green beads.

In conclusion, we have shown that the interplay between the effective stiffness and intrachain packing effects caused by side loops in polymers leads to novel helical equilibrium configurations of confined polymers. These structures are strikingly similar to ones recently observed in bacterial nucleoids. To what extent the physical effects discussed here are indeed able to explain the phenomenology of the large-scale chromosome organization in real bacteria is a question that clearly requires further research. At the very least, however, our results once again indicate that the ubiquitous aspecific interactions between the segments of long biopolymers like DNA can by themselves lead to significant spatial structuring, as has previously also been observed in the context of chromosome organization in the nuclei of plants [27] and humans [28]. This argues for a more prominent place for polymer physics in the research into the structure and function of chromosomes. From a purely physical point of view, our work points to novel possibilities for "sculpting" the configurations of confined polymers by judicial choices of polymer topologies.

We gratefully acknowledge discussions with Nancy Kleckner and Mara Prentiss (Molecular and Cellular Biology, Harvard) in the initial stages of this project. This work is part of the research program of the "Stichting voor Fundamenteel Onderzoek der Materie (FOM)," which is financially supported by the "Nederlandse Organisatie voor Wetenschappelijk Onderzoek (NWO)." The work of D. C. was supported by FOM-Program No. 103 "DNA in Action: Physics of the Genome."

*chaudhuri@amolf.nl, debc@iith.ac.in
†mulder@amolf.nl

[1] P.-G. de Gennes, *Scaling Concepts in Polymer Physics* (Cornell University, Ithaca, New York, 1979).
[2] *Polymer Handbook*, edited by J. Brandrup, E. H. Immergut, and E. A. Grulke (Wiley-Interscience, New York, 1999), 4th ed.
[3] D. J. Bonthuis, C. Meyer, D. Stein, and C. Dekker, Phys. Rev. Lett. **101**, 108303 (2008).
[4] J. Tang, S. L. Levy, D. W. Trahan, J. J. Jones, H. G. Craighead, and P. S. Doyle, Macromolecules **43**, 7368 (2010).

[5] H. Uemura, M. Ichikawa, and Y. Kimura, Phys. Rev. E **81**, 051801 (2010).
[6] D. Bates and N. Kleckner, Cell **121**, 899 (2005).
[7] S. Jun and B. Mulder, Proc. Natl. Acad. Sci. U.S.A. **103**, 12 388 (2006).
[8] P. Wiggins, K. Cheveralls, J. Martin, R. Lintner, and J. Kondev, Proc. Natl. Acad. Sci. U.S.A. **107**, 4991(2010).
[9] I. A. Berlatzky, A. Rouvinski, and S. Ben-Yehuda, Proc. Natl. Acad. Sci. U.S.A. **105**, 14 136 (2008).
[10] C. Butan, L. M. Hartnell, A. K. Fenton, D. Bliss, R. E. Sockett, S. Subramaniam, and J. L. S. Milne, J. Bacteriol. **193**, 1341 (2011).
[11] A. Maritan, C. Micheletti, A. Trovato, and J. R. Banavar, Nature (London) **406**, 287 (2000).
[12] S. B. Zimmerman, J. Struct. Biol. **156**, 255 (2006).
[13] P. Reiss, M. Fritsche, and D. W. Heermann, Phys. Rev. E **84**, 051910 (2011).
[14] H.-P. Hsu, W. Paul, S. Rathgeber, and K. Binder, Macromolecules **43**, 1592 (2010).
[15] H.-P. Hsu, W. Paul, and K. Binder, Macromolecules **43**, 3094 (2010).
[16] P. E. Theodorakis, H.-P. Hsu, W. Paul, and K. Binder, J. Chem. Phys. **135**, 164903 (2011).
[17] T. Birshtein, O. Borisov, Y. Zhulina, A. Khokhlov, and T. Yurasova, Polym. Sci. USSR **29**, 1293 (1987).
[18] J. D. Weeks, D. Chandler, and H. C. Andersen, J. Chem. Phys. **54**, 5237 (1971).
[19] H.-J. Limbach, A. Arnold, B. A. Mann, and C. Holm, Comput. Phys. Commun. **174**, 704 (2006).
[20] J. Hermans and R. Ullman, Physica (Amsterdam) **18**, 951 (1952).
[21] I. Kusner and S. Srebnik, Chem. Phys. Lett. **430**, 84 (2006).
[22] See Supplemental Material at http://link.aps.org/supplemental/10.1103/PhysRevLett.108.268305 for the details of the analysis of the center-of-mass distribution of the side loops around the main chain used in the construction of the effective potential described in the main text, as well as additional information on the structure function of the WLC chain model, and 4 additional snapshots of helical conformations at different conditions mentioned in the main text.
[23] P. G. Bolhuis, A. A. Louis, J. P. Hansen, E. J. Meijer, J. Chem. Phys. **114**, 4296 (2001).
[24] J. des Cloizeaux, J. Phys. (Paris) **36**, 281 (1975).
[25] M. Daoud, J. P. Cotton, B. Farnoux, G. Jannink, G. Sarma, H. Benoit, C. Duplessix, C. Picot, and P. G. de Gennes, Macromolecules **8**, 804 (1975).
[26] A. Y. Grosberg, P. G. Khalatur, and A. R. Khokhlov, Makromol. Chem. Rapid Commun. **3**, 709 (1982).
[27] S. de Nooijer, J. Wellink, B. Mulder, and T. Bisseling, Nucleic Acids Res. **37**, 3558 (2009).
[28] P. R. Cook and D. Marenduzzo, J. Cell Biol. **186**, 825 (2009).